Arch. Metall. Mater. **69** (2024), 3, 839-850

DOI: https://doi.org/10.24425/amm.2024.150904

M. SHAHIB AL BARI[1], JANUARTI J. EKAPUTRI[1*]

THE EFFECT OF FIBER ON THE GREEN STRENGTH AND BUILDABILITY OF HIGH-STRENGTH 3D PRINTING CONCRETE

Abstract. This paper presents four parameters in 3D Printing Concrete (3DPC) in the fresh state. Flowability, extrudability, open time, and buildability. In addition, this paper also introduces a new method to obtain the green strength of fresh concrete. The high-strength concrete mixture was used as a base mix design. The water to binder ratio and admixture were tuned to obtain the 3DPC that satisfied those four parameters. The 3DPC mix design used cement, silica fume, and reactive powder as a binder with a ratio of 3:1:1. The ratio of sand and binder was 0.9. The water to binder ratio (w/b) was 0.14 with the addition of a superplasticizer and accelerator. To increase the buildability, polyvinyl alcohol (PVA) fiber was added by 0.2% of concrete volume. It had a 30 mm slump, 110 mm flow, 1.1 SRF, 85 minutes of open time, and 7 KPa green strength in 75 minutes. This mix design was able to be printed into 40 layers of 100×400 mm cylinder.

Keywords: high-strength concrete; 3D printing; PVA fiber; green strength; shrinkage

1. Introduction

For the last decade, the application of additive manufacturing in construction industries has been a hot issue. This method implements industry 4.0 in construction, reducing time and eliminating formwork [1]. In this way, the characteristics of 3D Printing Concrete (3DPC) differ distinctively from normal concrete [2]. The printed mixture should retain its shape and withstand the layer load stacked on it. In addition, it should flow smoothly in the 3D concrete printer. Those characters are also influenced by their setting time when flowing and hardening.

Flowability is the ability to flow through pipes and extruders smoothly. However, there is no available standard to measure it. Tay suggested the slump and flow table test as the parameter of the flowability test [3]. The flow table test was included because it disturbs the mixture on top of the table by dropping the the table 25 times [4]. The disruption breaks the bonding or flocculation/coagulation process in fresh conditions to determine the flowability without clogging [5]. This test was also used by Zhang to determine the workability [6]. Another study introduced the shear vane test instead of slump test to determine the concrete workability because it represent rheological behavior better than the slump test by measuring the change of the shear stress over time [7]. However, this paper uses slump and slump flow tests for flowability parameter to approach the available concrete standard.

Extrudability is the ability of fresh concrete to flow continuously through the extruder while maintaining the shape quality. This parameter seems similar to flowability. However, maintaining the shape continuously when extruding is a different problem [8]. Some studies determined the extrudability by evaluating the quality of filament with visual observation [6,7,9]. However, it was unable to determine the value range to pass through the extruder smoothly. Panda introduced the shape retention factor (SRF) to quantify the filament's quality [10]. SRF is a ratio of nozzle diameter to filament width. It was recommended that the suitable SRF for 3DPC is 0.76-0.9 to achieve smooth filament after extrusion [11].

Buildability is the ability of a fresh concrete to maintain shape stability when the filament is loaded. Like flowability and extrudability, it has no standard. Zhang used concrete rheometer to obtain the rheological properties [6]. Kazemian used the cylinder stability test that is similar to compression test to determine the green strength [12]. Green strength is the minimum stress of material to deform during the fresh state. Wolfs conducted compression test using ASTM D2166 on fresh 3DPC at 15 and 30 minutes [13]. Due to the low stiffness, the optic measurement system was used to measure the strain. The fresh 3DPC

[1] DEPARTMENT OF CIVIL ENGINEERING, FACULTY OF CIVIL, PLANNING AND GEO ENGINEERING, INSTITUT TEKNOLOGI SEPULUH NOPEMBER, SURABAYA, 60111, INDONESIA

* Corresponding author: januarti@ce.its.ac.id

© 2024. The Author(s). This is an open-access article distributed under the terms of the Creative Commons Attribution-NonCommercial License (CC BY-NC 4.0, https://creativecommons.org/licenses/by-nc/4.0/deed.en which permits the use, redistribution of the material in any medium or format, transforming and building upon the material, provided that the article is properly cited, the use is noncommercial, and no modifications or adaptations are made.

is an anisotropic material that has different properties in each direction [14]. Practically, the 3DPC is printed layer by layer. Each filament should withstand the load of multiple filaments on top of it. Therefore, this study introduced the splitting tensile strength test from ASTM C496 to evaluate the green strength of fresh 3DPC. This test applies diametric compressive load along the length of filament until failure.

In addition to flowability, extrudability, and buildability, another important factor is open time. Open time is a duration when the mixture is printable in the fresh state [12]. After being mixed, it hardens over time which eventually clogs in the 3D concrete printer, Consequently, the printing time is limited. Although the open time is similar to the setting time test based on ASTM C403, the clogging often occurs before reaching the initial setting time [15]. This indicates that the duration of open time is shorter than the setting time. Accordingly, the printability limit and blockage limit were introduced as open time parameters [12].

Generally, the 3DPC eliminates casting in the formwork and compacting to build a structural component. It was inspired by the self-compacting concrete (SCC) and spray concretes (shotcrete) that remove the compacting process. Those two use high volumes of cementitious paste and admixtures [16]. It fills smooth-graded aggregate particles to create high flowability in SCC. However, this concrete requires formwork that demands the time and cost to install it. Meanwhile, the shotcrete was extruded with high pressure to cast it on the vertical surface. Similar to SCC, the shotcrete requires high amount of cementitious paste and high amount of accelerator to enhance the bond on the surface [17,18]. These mixes often achieve high compressive strength that inspired some studies to use the high-performance concrete (HSC) for 3DPC. Özalp used 800 kg/m^3 of cement with 0.3 water to binder ratio that achieved 60 MPa compressive strength at 28 days on 100×100×100 mm cube [19]. The cube specimen was cut from the stacked layer and tested on three direction which achieved similar value. The HSC provided high interlayer adhesion between two layers. Le obtained a well printed stacked layers using a HSC that achieved 102 MPa compressive strength at 28 days [20]. Gosselin also recommended to use ultra-high-performance concrete (UHPC) as a 3DPC to create a challenging geometrical structure [21]. Therefore, this study used HSC as a basic composition to obtain the 3DPC mix design.

A HSC used silica fume and reactive powder to enhance its strength [22]. It also used 0.9 silica sand to binder ratio. Silica fume is an amorphous byproduct material that has high silica content [23]. Meanwhile, the reactive powder is an amorphous pozzolanic material that has high silica content and fine particle [24]. It has higher pozzolanic reactivity than silica fume [25]. Both materials enhance strength and durability of concrete with or without special treatment [26-28]. It is mandatory to use these materials to achieve high compressive strength and durability [29,30].

The weakness of HSC is its high shrinkage due to the very low water to binder ratio (w/b) and high cement content [31]. When the concrete is cured, the water is absorbed by the hydration reaction which is called self-desiccation [32]. It reduces the relative humidity and leaves the void on fine capillaries. Thus, inward stress occurs causing autogenous shrinkage [33]. This shrinkage has a high correlation with the relative humidity inside the concrete which continually lowers over time [34]. While the autogenous shrinkage is relatively small, lower w/b inside the concrete can visibly shrink the cross-section of the specimen.

The main purpose of polyvinyl alcohol (PVA) fiber in concrete is to reduce the crack of concrete [35]. its dispersion gives dense distribution inside the concrete matrix that resists the tensile load controlling the propagation of micro-cracks and increasing the tensile strength of concrete [36]. This capability has a potential to improve the green strength of fresh concrete increasing buildability. However, the tensile modulus is decreased when the PVA fiber is added to more than 0.3%. Besides, increasing its volume fraction drops the workability [37]. Accordingly, this study uses PVA fiber by 0.2% volume fraction of concrete to limit its effect on flowability. In addition, it has less than 1% of water absorption [38].

A HSC mix design from a previous study that had a 128 MPa compressive strength at 28 days was selected as a base composition [22]. It had high early strength which is necessary to retain its shape and support stacked layers during its fresh state [7]. It also had high workability. This paper adjusts the HSC as a 3DPC material using four parameters that were measured with ASTM standard test to determine its compatibility with a 3D concrete printer.

2. Materials and mix design

Four mixtures used in this study are presented in TABLE 1 with the HSC as a base. The chemical content of Portland cement, silica fume, reactive powder and silica sand is presented in TABLE 2. PVA fiber by 0.2% of the concrete volume was added. It had a 42 μm diameter, 8 mm length, and specific gravity of 1.3 gr/cm^3. It also had a tensile strength of 1600 MPa, flexural strength of 40 GPa, and less than 1% water absorption. Then, the performance of 3DPC was examined with early compressive strength, splitting tensile strength, and shrinkage.

TABLE 1

Mix design with different w/b

Material	Mix Design (kg/m^3)			
	HSC	W14	W14F*	W16
Portland cement	712	712	712	712
Silica fume	231	231	231	231
Reactive powder	211	211	211	211
Silica sand	1020	1020	1020	1020
Superplasticizer	31	31	31	31
Accelerator	30	30	30	30
Water	129	162	162	185
PVA fiber	—	—	2.58	—
Total	2,364	2,396	2,399	2,420
w/b	0.11	0.14	0.14	0.16

TABLE 2

Composition of each material

Parameter	Chemical content (%)			
	Cement	Silica fume	Glass powder	Silica sand
Silicon dioxide (SiO_2)	19.19	81.4	71.73	99.05
Iron (III) oxide (Fe_2O_3)	3.11	9.3	0.54	0.04
Aluminum oxide (Al_2O_3)	5.42	—	1.73	0.21
Calcium oxide (CaO)	63.08	—	7.87	0.02
Magnesium oxide (MgO)	1.77	—	4.59	0.05
Sodium oxide (Na_2O)	0.22	9.3	12.45	0.02

The mix design was determined to comply with the sequence of tests in a flowchart in Fig. 1. Those tests approach the ASTM standard to determine the characteristic of 3DPC on a 3D concrete printer. There are four parameters: flowability, extrudability, open time, and buildability. Extrudability is the most crucial part because the 3DPC has to be printable out of an extruder smoothly. However, each study has its own extruder design that provided different parameter [2,3,7,13,39].

The flowability test was conducted using slump and flow table tests according to ASTM C1437 and C143, respectively [4,40]. The slump test used a mini slump cone which has a scale of ¼ standard cone as presented in Fig. 2. This was set to approximate the actual filament size. Meanwhile, the flow table test used a standard flow table following ASTM C230 [41]. The parameter followed Tay's result which had a 4-8 mm slump from a 50 mm height cone and 150-190 mm slump flow [3].

A mini 3D concrete printer shown in Fig. 3 was used for the extrudability, open time, buildability, and printing tests. It has a size of 1×1×1 m. Its printing range is 500×500×400 mm. The extruder consists of a feeder and Archimedes screw that is attached on the x-axis. The cylinder nozzle has a diameter in the range of 20-40 mm. The maximum printing speed and angular velocity of the screw were 10 mm/s and 80 rpm. Before conducting the printing, the 3DPC was mixed first using 7 L professional mixer machine for 20 minutes. After cooling down for 10 minutes, it was inserted to the feeder.

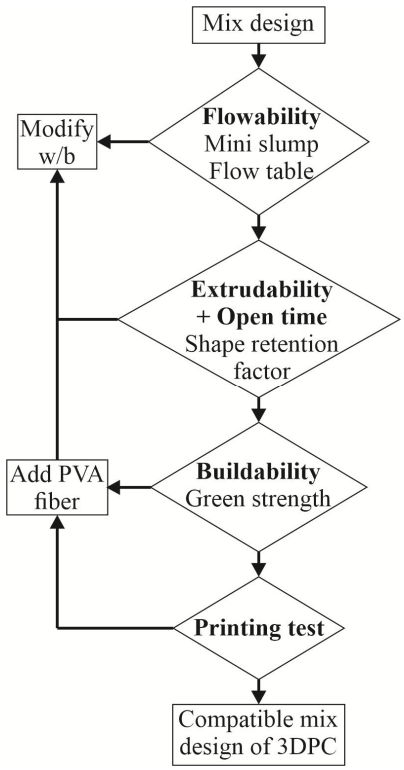

Fig. 1. A flowchart for finding the mix design of 3DPC conforming to the current standard

The extrudability used the SRF test to examine the quality of filament and the open time. The SRF test was performed directly on a mini 3D concrete printer to determine the compatibility of the mixture with the extruder. The SRF is the ratio of the nozzle's diameter and layer's width that is extruded out of a 3D concrete printer [10]. The printing speed and angular velocity of the screw were 10 mm/s and 80 rpm. To examine the SRF, this study used a 20 mm cylinder nozzle. The concrete was printed as presented in Fig. 4. Then, the width of three long horizontal filaments was measured using the Vernier scale. This experiment was repeated every 5 minutes until the clogging occurred or the filament was discontinuous that indicated the end of the test.

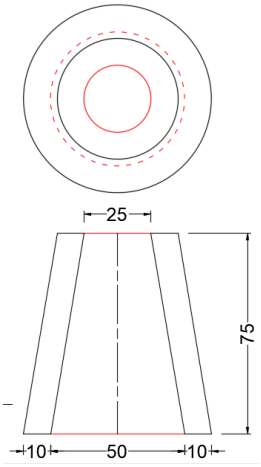

(a) Mini slump design in mm

(b) Actual mini slump

Fig. 2. Mini slump

Fig. 3. A 1×1×1 m 3D concrete printer

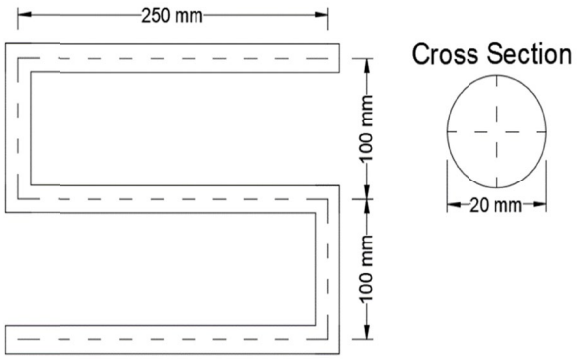

Fig. 4. Design of filament for SRF test

The open time was obtained from the SRF test. It measured the duration of printable 3DPC. The duration was calculated from the start of the mixing until the discontinuous filament was occurred. Then, the result was compared with the penetrometer test which was conducted according to ASTM C403 [42]. The mixture was cast into the mold with a size of 15×15×15 cm. The penetrometer was pricked on the surface of the concrete every 15 minutes.

The buildability test consists of green strength that is not simple to perform as the concrete is in a fresh state. This paper introduces a new way of measuring the green strength on fresh concrete using a simple instrument which is adopted form splitting tensile strength from ASTM C496 [43]. The diametric compressive load along the length induces tensile stresses on the plane containing the applied load. The loaded areas are in a state of longitudinal direction rather than uniaxial compression making the tensile failure occur. It allows them to resist higher compressive stresses than would be indicated by the uniaxial compression test result. The tensile failure on fresh concrete is indicated by how much the deformation is allowed. The tensile stress that retains the shape until the determined deformation is called the green strength. The setting of the green strength instrument is presented in Fig. 5.

The fresh concrete was extruded from a 3D concrete printer through a 40 mm nozzle. The maximum printing speed and angu-

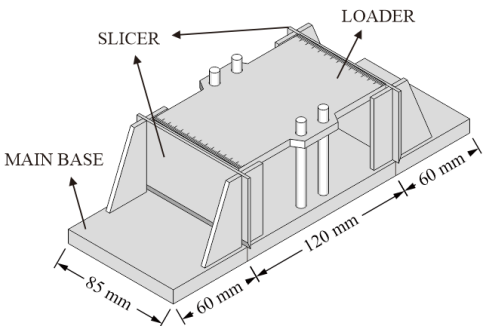

(a) Component of green strength

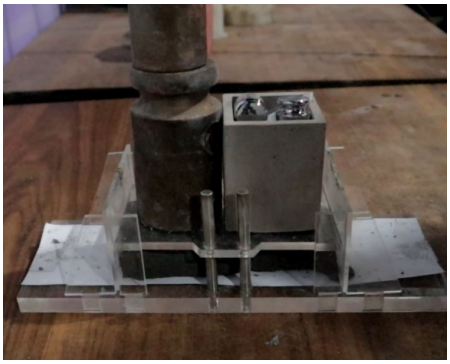

(b) Ballast loaded the filament

(c) Measuring width using Vernier scale

Fig. 5. Green strength instrument

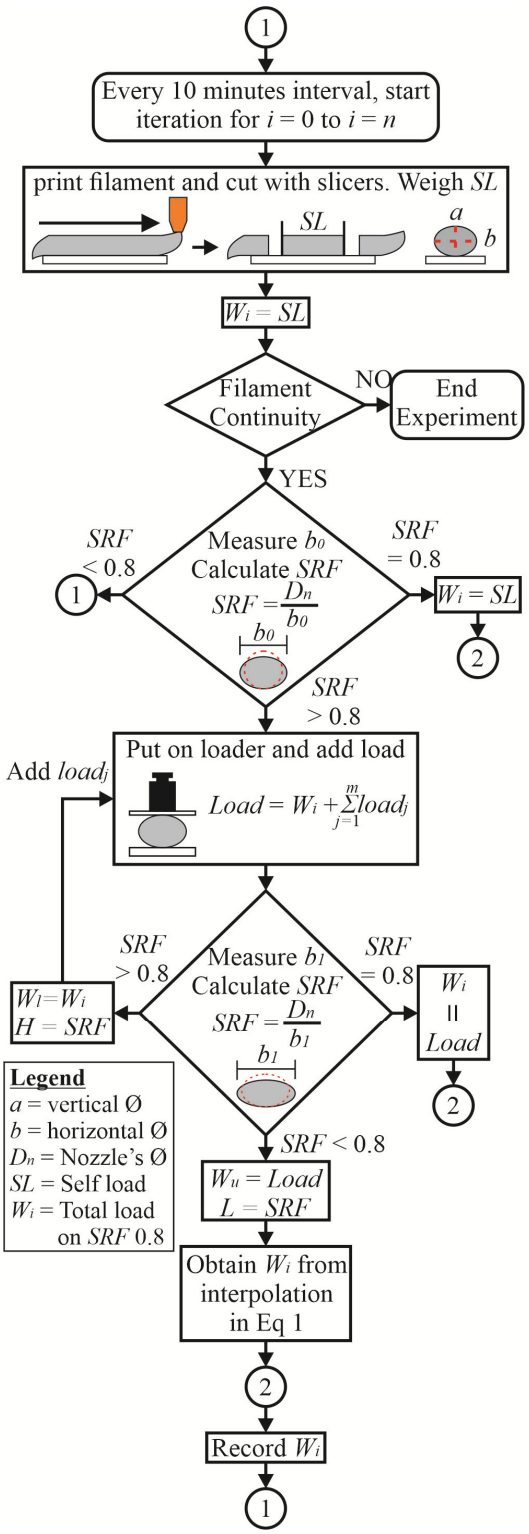

Fig. 6. Sequence for measuring green strength

lar velocity of the screw were 3 mm/s and 80 rpm. The concrete was printed longitudinally on the instrument shown in Fig. 5(a). The slicers cut and constrain both ends of 120 mm long filament. Then the filament was loaded as shown in Fig. 5(b). The procedure for measuring the green strength of fresh concrete is shown in Fig. 6. It obtains the total load W_i on 0.8 SRF. The range 0.8 was used as a deformation limit of filament width following the minimum SRF that was recommended by Panda [10]. If the W_i is not acquired, it can be interpolated with WU and W_L as presented in Fig. 7 using Eq. (1). Then, W_i is used to calculate the green strength of fresh concrete with Eq. 2. This equation divides the load into diametrical stress of ellipse along the length.

$$W_i = (W_u - W_l) \times \frac{(0.8 - L)}{(H - L)} \tag{1}$$

Where:

W_i – Load on 0.8 SRF,
W_u – Load when SRF less than 0.8 (overload),
W_L – Load when SRF is more than 0.8 (under load),
H – SRF when under load,
L – SRF when overload.

$$f_{green} = \frac{4W_i}{\pi.L.(a+b)} \tag{2}$$

Where:

f_{green} – Green strength,
W_i – Load o0.8 SRF,
L – Length of filament,
a – Vertical diameter of the ellipse of filament cross-section,
b – Horizontal diameter of the ellipse of filament cross-section.

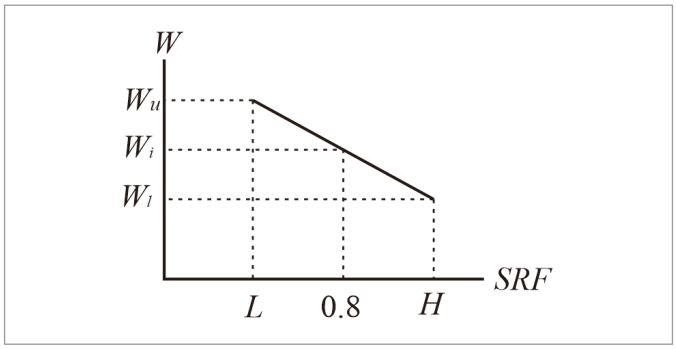

Fig. 7. Interpolation of Wi on 0.8 SRF

After obtaining the qualified mix design, the concrete was printed into a 100×400 mm cylinder shell. The printing process was conducted at ambient temperature which was 32°C. Each layer had a height of 10 mm and a width of 20 mm; thus, 40 layers were required. The printing method was layer by layer that prints a complete layer before the head printer rise at the z-axis. The printing speed and angular velocity of the screw were 10 mm/s and 80 rpm, respectively. The printing test started at 30 minutes after mixing.

After obtaining the suitable mix design, the mechanical properties of suitable concrete were analyzed. The test of compressive strength, splitting tensile strength, and shrinkage were conducted. The early compressive strength was used to obtain 3DPC performance in an early state. It was conducted following ASTM C39 [44]. The test specimen was a 50×100 mm cylinder. The early compressive strength test was conducted for up to

24 hours. The samples were immediately tested as soon as the samples were able to be extracted from the mold. The test instrument with a capacity of a 500 KN universal testing machine (UTM) was used for the mechanical test.

The splitting tensile strength test used the same mold and testing machine. This test was compared with the green strength test which originated from it. The test was conducted 24 hours following ASTM C496 after the concrete was cast [43].

The shrinkage test was conducted following the previous study which used a strain gauge embedded into the center of the concrete cylinder [34]. The change of length was recorded by the data logger every 30 seconds interval. The HSC was molded into a 50×100 mm cylinder. The polytetrafluoroethylene (Teflon) sheet was inserted between the mixture and the mold to allow the concretes to move without restraint. A 3 cm long embedded strain gauge type KM-30-120-H1-11Y3M2 with a resistance of 120Ω ± 1% was used. The strain gauge was inserted into the center of the cylindrical specimen immediately when the mixture was molded. The shrinkage setup is presented in Fig. 8. Then, the mold was closed tightly to ensure the measurement was in sealed condition without the influence of external moisture during hardening. The room temperature was kept constant at 20°C when the concrete hardens in less than a day, the mold was dismantled to measure the concrete shrinkage without curing. The shrinkage was conducted for 7 days.

3. Results and discussions

The flowability results which consisted of a slump and flow table test are presented in Fig. 9. The higher w/b the higher the slump (marked in red dots) and flow table (marked as bars). However, adding PVA fiber reduced slump value and flow diameter. Based on Tay's, the optimum flow table for printing was 150-190 mm [3]. The slump was recommended to reach 0 mm to achieve shape stability of solid-like filament. However, no sample achieved a 0 mm slump. The nearest sample was HSC which was 15 mm. the change of w/b increased workability only. Adding PVA fiber on W14F slightly decreased the slump because of the increasing viscosity [36].

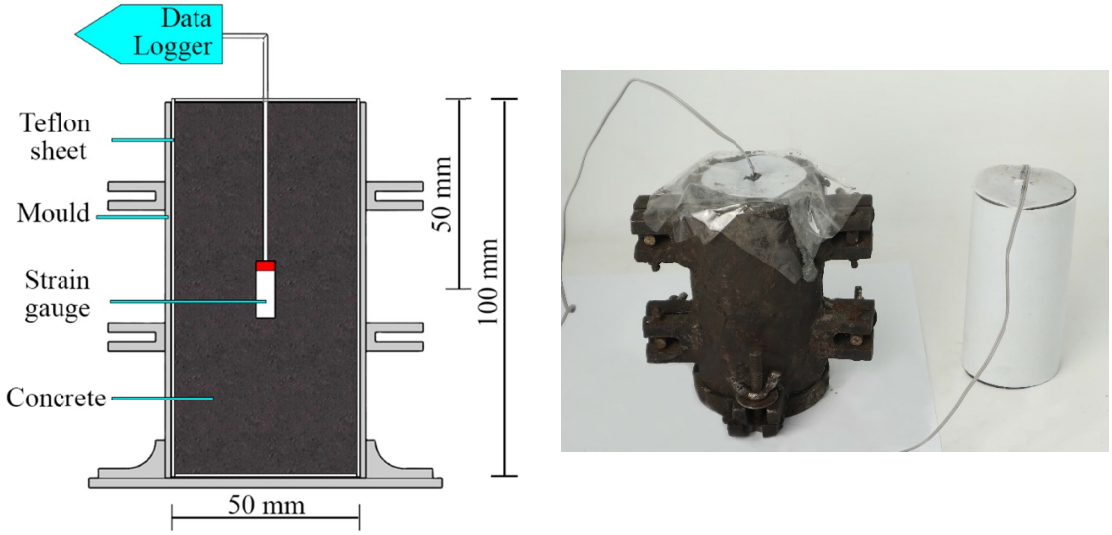

(a) specimen setup (b) an actual specimen in mold

Fig. 8. shrinkage test

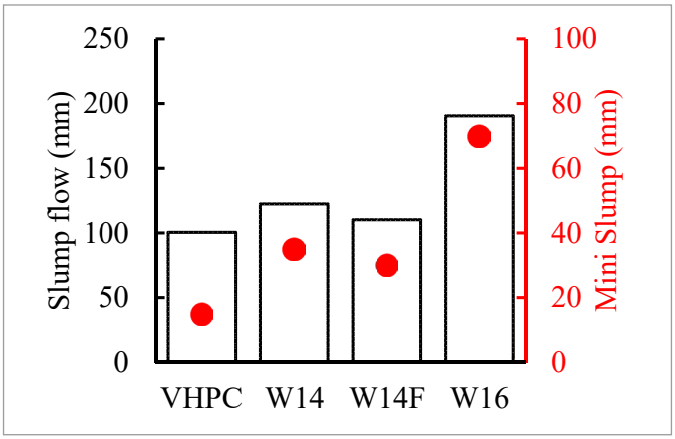

Fig. 9. Mini slump and flow table test result

SRF test was conducted and placed side by side in Fig. 10 to determine the effect of a mini slump on SRF. Mini slump presented shape stability by holding its own weight. However, the low slump in HSC, which was 15 mm, clogged the printer causing the discontinuous filament. W14 had a 35 mm slump that produced smooth filament. Adding 0.2% PVA fiber only reduced slump by 5 mm that also had smooth filament. W16 had the highest slump, which was 70 mm, but unprintable because it was too flow. Tay recommended that 4-8 mm of 50 mm cone was the optimum slump flow for 3DPC, which is close to zero slump [3]. This study found that 30-35 mm of 75 mm mini cone was sufficient to produce smooth SRF, thus W14 and W14F were selected. It also found the compatibility of 3DPC by printing it directly on 3D concrete printing.

(a) Mini slump of HSC (15 mm)

(b) SRF of HSC

(c) Mini slump of W14 (35 mm)

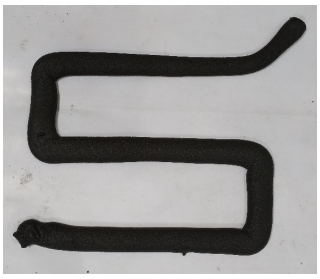

(d) SRF of W14

(e) Mini slump of W14F (30 mm)

(f) SRF of W14F

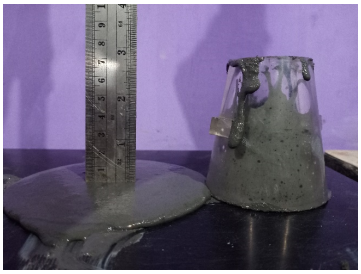

(g) Mini slump of W16 (75 mm)

(h) SRF of W16

Fig. 10. The connection of mini slump and SRF form of each sample

The selected mix designs were tested every 5 minutes to observe how long the filament quality last which is presented in Fig. 11. The SRF of W14 was 0.79 at 35 minutes. It had smooth printed filament which could be repeated for up to 110 minutes before clogging. W14F had a shorter printability time than W14, which was 85 minutes. The Each final open time was determined by the discontinuity of filament that occurs on the next 5 minutes interval. Its SRF in the range of 1.1-1.2 means that the width of the filament was shorter than the nozzle diameter. The filament did not flatten by self-load indicating that W14F had higher load resistance than W14. Meanwhile, W16 was unprintable due to SCC characteristics which flowed out continuously from 3DPC.

All SRF result had the range of 0.73-1.2 and was printable on the 3D printer. This result differs from another study that rec-

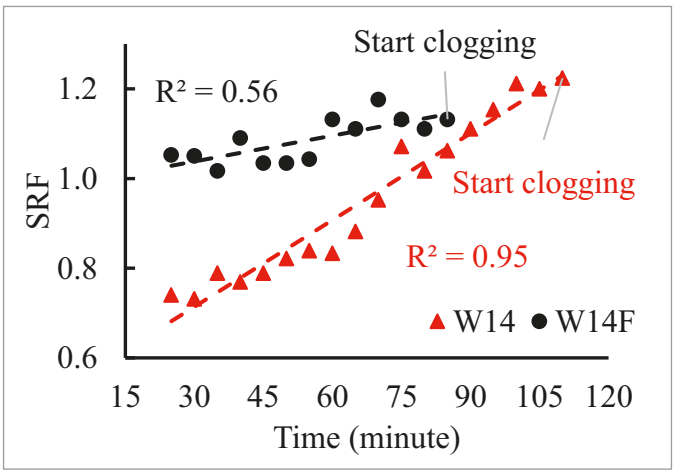

Fig. 11. Shape retention factor of W14 and W14F

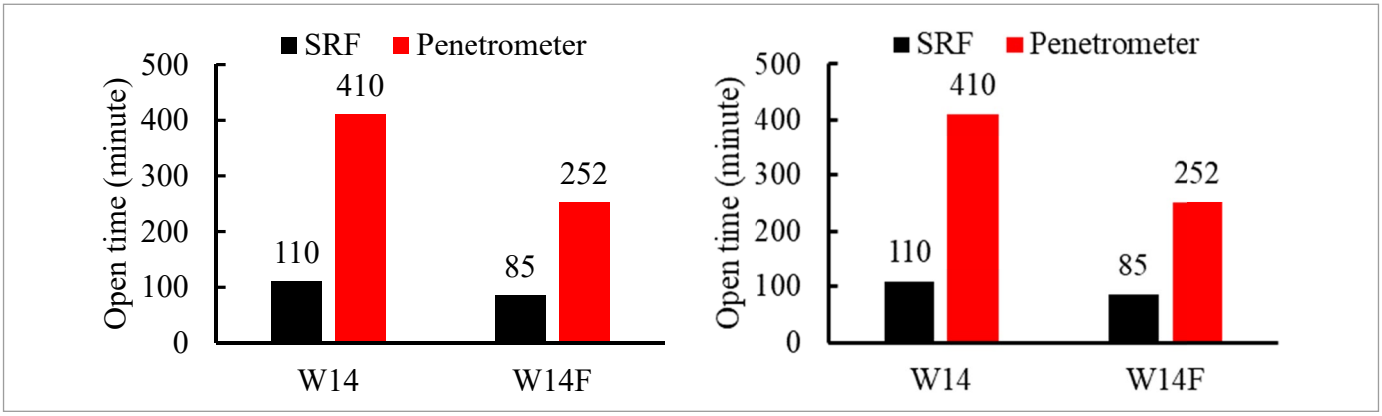

Fig. 12. Comparison of open time between SRF and penetrometer result

ommended the optimum SRF range was 0.76-0.91 [11]. It points out that SRF is determined by the specification of a 3D printer.

The comparison of the open time of SRF and penetrometer is presented in Fig. 12. The initial setting time of the penetrometer was longer than SRF. The shorter time of W14F than W14 was caused by PVA fiber that increased viscosity and reduced workability [36]. The penetrometer was unable to represent the open time better than the actual test on the 3D printer due to its long initial setting time. This result was in accordance with Kazemian's that found no correlation between open time and setting time [12]. Therefore, it is recommended to use the SRF test to determine the open time of the 3DPC mixture.

The green strength test of W14 and W14F presented in Fig. 13 gradually increased over time. Adding PVA fiber rapidly increases the green strength of fresh concrete due to its ability to withstand the filament splaying. In addition, PVA fiber increases the tensile and splitting strength of concrete as well as prevents the cracks caused by the autogenous shrinkage [32]. In a fresh concrete, the PVA fiber also increases green strength providing the ability to retain the shape of fresh concrete and increase the load resistance. Those results stopped at 75 minutes because the filaments were discontinuous during printing. The test time was stopped before the open time because of different nozzle diameter. Bigger filament diameter caused early clogging due to the big volume extruded on the constant screw speed although the printing speed was reduced. Thus, the 3D printer of this study was capable to flow out the fresh concrete with the green strength up to 7 KPa in 75 minutes.

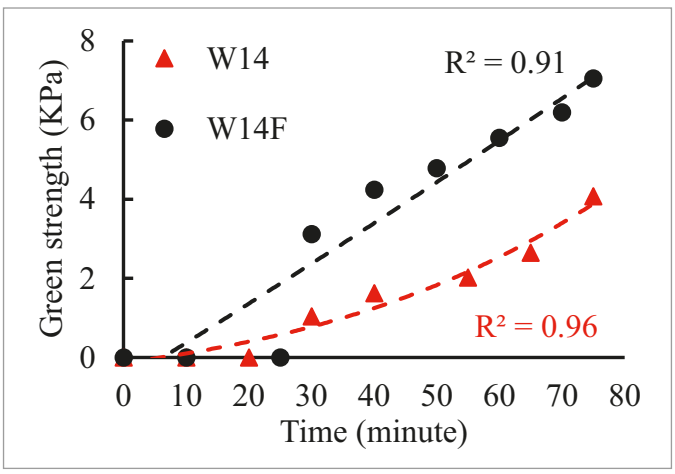

Fig. 13. Green strength of W14 and W14F

The early compressive strength result is presented in Fig. 14. W14 achieved 0.4 MPa of compressive strength in 5 hours. In 24 hours, its compressive strength reached 18.6 MPa. Despite the reduced compressive strength in one day due to the increase of w/b, W14 had high early compressive strength which potentially withstands the load of the upper filament. The silica fume and reactive powder also gave a huge contribution to the high early strength [45]. reactive powder is an amorphous material that increases calcium silicate hydrate (C-S-H) reaction [46].

Despite high compressive strength at early age, it is not associated directly with the green strength of the filament. PVA fiber in W14F reduced the compressive strength by up to 15%. At an early age, the 0.2% PVA fiber slightly reduced the compressive strength. However, a previous study found that adding PVA fiber increased the compressive strength at a later age [36].

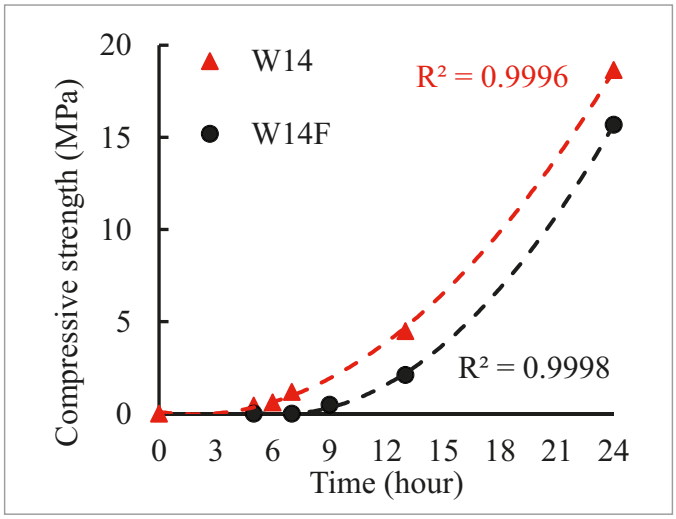

Fig. 14. Early compression test of W14 and W14F

The splitting tensile strength test result expressed in Fig. 15 shows that adding PVA fiber increased the splitting tensile

strength. In the fresh state, adding PVA fiber increased the green strength at 75 minutes by 43%. In addition to a tensile load resistance, it increased the shape retention which showed on its SRF in the range 1.1-1.2. This range presents that the width of the filament was smaller than the nozzle.

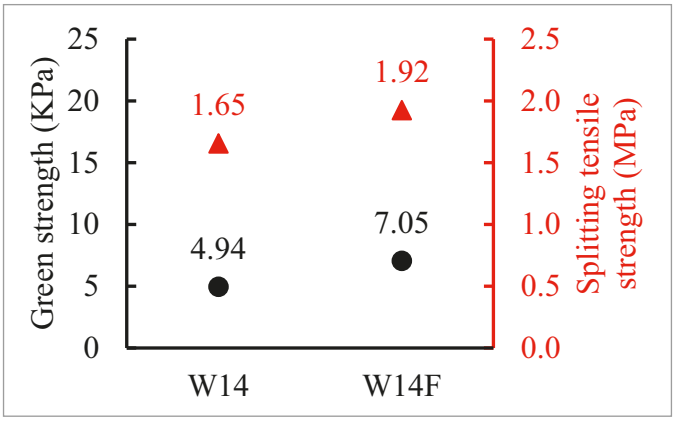

Fig. 15. Comparison of green strength at 75 minutes and splitting tensile strength at one day of W14 and W14F

The printing test result of W14 and W14F is presented in Fig. 16. W14 (left) only produced 18 layers and 140 mm in height. Many cracks that appeared on the underlayers were caused by the shrinkage and worsened by the self-load on it. The shrinkage was caused mainly by autogenous shrinkage but worsened by drying shrinkage because the printed layers were exposed to ambient temperature. The underlayers were compressed which indicated that the green strength was not enough to retain the shape and withstand the load. The upper layers had big filaments caused by the high standoff between the printed layer and the nozzle that distorted the shape. W14F (right) using PVA fiber greatly reduced the cracks and increase its green strength which printed 40 layers of 100×400 mm cylinder shell in 22 minutes successfully. PVA fiber increased green strength that provided a consistent shape throughout all layers. This result confirms with another studies that fiber is required to enhance the performance of the filament [7,11,47].

Fig. 16. Printing test results of W14 (left) and W14F (Right)

The printing test was conducted for 22 minutes. In addition of 30 minutes from the mixing, the total open time conducted was 52 minutes. It was lower than actual open time of each sample in Fig. 12. The open time was limited due to the height limit at z-axis of 3D concrete printer which was 400 mm. W14F was possible to print more layers as it has remaining open time by up to 85 minutes.

The shrinkage test measures the longitudinal change of shrinkage on the specimen. Fig. 17 is the shrinkage test results on closed and open condition. In the closed condition, W14 shrank up to 900×10^{-6} in 10 hours, while W14F was 800×10^{-6}. This phenomenon is called the autogenous shrinkage which commonly occurs on the concrete with low w/b due to the chemical reaction at an early age [33]. Moreover, because of low w/b, the autogenous shrinkage is increased by self-desiccation. It occurs when the water is absorbed by cement hydration which lowers the humidity of concrete pores causing the microcrack to emerge [32]. This microcrack was caused by developed inner tensile stresses resulting in significant contraction [31]. After demolding, W14 fell into 2200×10^{-6} in 20 hours, while W14F was 2000×10^{-6}. The difference even gets larger in seven days between these two mixtures, where the highest shrinkage of W14 and W14F are 2800×10^{-6} and 2400×10^{-6}, respectively. After demolding, the shrinkage was larger because of the concrete was exposed to open air without curing that greatly reduced the concrete moisture.

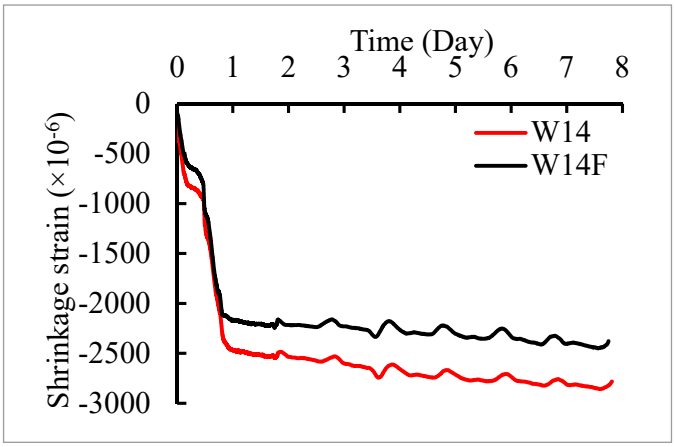

Fig. 17. Shrinkage test result of W14

This high shrinkage of W14 is the main problem that appeared in the printing result in Fig. 16. While its green strength was low, the cracks on the exposed filament were appeared immediately before the concrete sets. Adding PVA fiber greatly reduced the shrinkage, which is the main purpose of using the fiber [48]. It also increased the green strength preventing the un-

derlayer from cracking and reducing deformation when stacking.

3DPC mix design in this paper was obtained by modifying HSC from a previous study that achieved 57 MPa and 128 MPa of compressive strengths at 1st and 28th days, respectively [22]. Based on the test results it was found that W14F was the suitable mix design that was printed 100×400 mm cylinder shell successfully. It had a 30 mm slump, 110 mm flow, 3 KPa of green strength in 30 minutes, and 85 minutes of open time. It achieved 15 MPa in a day although it was lower than W14.

Even though W14 had smooth filament during the SRF test, it failed to print because of a flattened underlayer due to insufficient green strength. Using equation 1, a 10×20 mm layer had a load of 0.16 KPa, which in total was 6.4 KPa that printed in 22 minutes. During the same start time, which was 30 minutes, the concrete should sustain this load after 50 minutes. W14 only had 2 KPa while W14F had 4.8 KPa. This great distinction caused the underlayer of W14 to flatten causing a standoff with the nozzle and disorienting extruded layer.

This suggested sequence provided the capability of a 3D concrete printer. In extrudability, this printer was able to print the concrete with the slump up to 30 mm and slump flow up to 110 mm as presented in Fig. 10(e) and (f), which is different from Tay's parameter. The buildability parameter determines the minimum strength required for 3DPC to sustain the load on the printing test. It also determines the 3D printer limit such as W14F that clogged the extruder at 70 minutes resulting in 7 KPa of green strength as the limit. W14, however, was stopped due to the discontinuous filament. It also indicated that the 3D printer can print more mix design variation that satisfies the parameters.

4. Conclusions

Herein, a 3DPC material obtained from the suggested sequence has been discussed. The most critical factor was the SRF test, which determines the ability of 3DPC to be extruded before determining its performance. Then, the green strength determines the load capacity of the fresh concrete. Here is the summary of this study.

1. The 3DPC mix design consisted of cement, silica fume, and reactive powder as a binder with a ratio of 3:1:1. The ratio of sand and binder was 0.9. The water to binder ratio (w/b) was 0.14 with the addition of a 4% superplasticizer and 4% accelerator. 0.2% polyvinyl alcohol (PVA) fiber was added by concrete volume.
2. This suggested sequence uses four parameters which are flowability, extrudability, open time, and buildability. Flowability consists of a mini slump and flow table tests. Extrudability and open time use SRF test. Buildability uses a green strength test. It determined each test parameter for mini 3D concrete printing with Archimedes screw attached directly to the extruder. The maximum slump was 35 mm. The slump flow range was 110-150 mm. The printable SRF was 0.8-1.2. The maximum green strength was 7 KPa obtained in 75 minutes.
3. A method how to measure the green strength test was proposed. This test uses a simple instrument that is adopted from the splitting tensile strength test from ASTM C496. The green strength of fresh concrete is measured based on the deformation of filament at SRF of 0.8.
4. Water to binder ratio controlled the flowability of 3DPC. However, it was unable to achieve good extrudability and green strength. It is required to insert additional material to enhance its performance.
5. The open time using SRF as compared with setting time with a penetrometer. There was no correlation between these two methods. Therefore, it is recommended to determine the open time on the 3D concrete printer directly.
6. The mechanical property of 3DPC was determined by buildability as one of the parameters. However, only green strength represents its property. The recommended green strength formula in this paper can be used as a benchmark to determine the strength of fresh concrete.
7. The effect of PVA fiber in the printing test of a 100×400 mm cylinder was observed. Concrete without fiber produced only 18 layers and 140 mm in height with cracks on under layers. Adding fiber repaired the mixture which achieved 40 layers and 400 mm height successfully. The fiber reduced the shrinkage and enhanced the green strength because of its ability to increase tensile strength controlling the propagation of micro-crack. However, it decreased the open time and compressive strength at an early age.
8. The autogenous shrinkage of W14 and W14F occurred at 900×10^{-6} and 800×10^{-6} in 10 hours, respectively. When the concrete was exposed, the shrinkage fell to 2400×10^{-6} and 2100×10^{-6}, respectively. This shrinkage was caused by the low water/binder ratio, which was only 0.14. The great shrinkage in open condition resulted apparent crack on the printed W14. Alternatively, the fiber enhanced the green strength and reduced the shrinkage producing the smooth filaments on the printed W14F.

Acknowledgments

The research described in this paper was financially supported by the Direktorat Riset, Teknologi, dan Pengabdian Masyarakat (DRPM-ITS), Kementerian Pendidikan, Kebudayaan, Riset dan Teknologi Republik Indonesia [contract number 008/E5/PG.02.00PT/2022 and sub-contract no. 1513/PKS/ITS/2022]. The authors also gratefully acknowledge financial support from the Institut Teknologi Sepuluh Nopember for this work, under project scheme of the Publication Writing and IPR Incentive Program (PPHKI) 2022. The authors express gratitude to the BASF Indonesia for providing accelerator. We also thank SIKA for providing the silica fume.

REFERENCES

[1] S.C. Paul, G.P.A.G. van Zijl, I. Gibson, A review of 3D concrete printing systems and materials properties: current status and fu-

ture research prospects. Rapid Prototyp. J. **24**, 4, 784-798 (2018). DOI: https://doi.org/10.1108/RPJ-09-2016-0154

[2] G.P.A.G. Van Zijl, S.C. Paul, M.J. Tan, Properties of 3D printable concrete. In Proceedings of the International Conference on Progress in Additive Manufacturing Part F1290, 421-426 (2016).

[3] Y.W.D. Tay, Y. Qian, M.J. Tan, Printability region for 3D concrete printing using slump and slump flow test. Compos. Part B Eng. **174**, 106968 (2019). DOI: https://doi.org/10.1016/j.compositesb.2019.106968

[4] ASTM International, ASTM C1437-15: Standard Test Method for Flow of Hydraulic Cement Mortar., pp. 7-8 (2015).

[5] R.D. Ferron, S. Shah, E. Fuente, C. Negro, Aggregation and breakage kinetics of fresh cement paste. Cem. Concr. Res. **50**, 1-10 (2013). DOI: https://doi.org/10.1016/j.cemconres.2013.03.002

[6] Y. Zhang, Y. Zhang, W. She, L. Yang, G. Liu, Y. Yang, Rheological and harden properties of the high-thixotropy 3D printing concrete. Constr. Build. Mater. **201**, 278-285 (2019). DOI: https://doi.org/10.1016/j.conbuildmat.2018.12.061

[7] T.T. Le, S.A. Austin, S. Lim, R.A. Buswell, A.G.F. Gibb, T. Thorpe, Mix design and fresh properties for high-performance printing concrete. Mater. Struct. Constr. **45**, 8, 1221-1232 (2012). DOI: https://doi.org/10.1617/s11527-012-9828-z

[8] M.G. Wei, W. Li, J. Yang, State-of-the-art of 3D printing technology of cementitious material – An emerging technique for construction. Sci. China Technol. Sci. **60**, (2017). DOI: https://doi.org/10.1007/s11431-016-9077-7

[9] A.V. Rahul, M. Santhanam, H. Meena, Z. Ghani, 3D printable concrete: Mixture design and test methods. Cem. Concr. Compos. **97**, 13-23 (2019). DOI: https://doi.org/10.1016/j.cemconcomp.2018.12.014

[10] B. Panda, M.J. Tan, Experimental study on mix proportion and fresh properties of fly ash based geopolymer for 3D concrete printing. Ceram. Int. **44**, 9, 10258-10265 (2018). DOI: https://doi.org/10.1016/j.ceramint.2018.03.031

[11] F. Özalp, H.D. Yilmaz, Fresh and Hardened Properties of 3D High-Strength Printing Concrete and Its Recent Applications. Iran. J. Sci. Technol. – Trans. Civ. Eng. **44**, 319-330 (2020). DOI: https://doi.org/10.1007/s40996-020-00370-4

[12] A. Kazemian, X. Yuan, E. Cochran, B. Khoshnevis, Cementitious materials for construction-scale 3D printing: Laboratory testing of fresh printing mixture. Constr. Build. Mater. **145**, 639-647 (2017). DOI: https://doi.org/10.1016/j.conbuildmat.2017.04.015

[13] R.J.M. Wolfs, F.P. Bos, T.A.M. Salet, Early age mechanical behaviour of 3D printed concrete: Numerical modelling and experimental testing. Cem. Concr. Res. **106**, 103-116 (2018). DOI: https://doi.org/10.1016/j.cemconres.2018.02.001

[14] J. Ye, C. Cui, J. Yu, K. Yu, J. Xiao, Fresh and anisotropic-mechanical properties of 3D printable ultra-high ductile concrete with crumb rubber. Compos. Part B Eng. **211**, no. September 2020, 108639 (2021). DOI: https://doi.org/10.1016/j.compositesb.2021.108639

[15] H. Alghamdi, S.A.O. Nair, N. Neithalath, Insights into material design, extrusion rheology, and properties of 3D-printable alkali-activated fly ash-based binders. Mater. Des. **167**, 107634 (2019). DOI: https://doi.org/10.1016/j.matdes.2019.107634

[16] N. Gowripalan, P. Shakor, P. Rocker, Pressure exerted on formwork by self-compacting concrete at early ages: A review. Case Stud. Constr. Mater. **15**, July, e00642 (2021). DOI: https://doi.org/10.1016/j.cscm.2021.e00642

[17] N. Banthia, Advances in sprayed concrete (shotcrete), in Developments in the Formulation and Reinforcement of Concrete. Elsevier LTD, pp. 289-306 (2019).

[18] V.M. de Alencar Monteiro, F. de Andrade Silva, On the design of the fiber reinforced shotcrete applied as primary rock support in the Cuiabá underground mining excavations: A case study. Case Stud. Constr. Mater. **15**, no. November (2021). DOI: https://doi.org/10.1016/j.cscm.2021.e00784

[19] F. Özalp. H.D. Yilmaz, Fresh and Hardened Properties of 3D High-Strength Printing Concrete and Its Recent Applications. Iranian Journal of Science and Technology – Transactions of Civil Engineering (2020). DOI: https://doi.org/10.1007/s40996-020-00370-4

[20] T.T. Le et al., Hardened properties of high-performance printing concrete. Cem. Concr. Res. **42**, 3, 558-566 (2012). DOI: https://doi.org/10.1016/j.cemconres.2011.12.003

[21] C. Gosselin, R. Duballet, P. Roux, N. Gaudillière, J. Dirrenberger, P. Morel, Large-scale 3D printing of ultra-high performance concrete – a new processing route for architects and builders. Mater. Des. **100**, 102-109 (2016). DOI: https://doi.org/10.1016/j.matdes.2016.03.097

[22] A.D. Agustin, J. J. Ekaputri, Very High Performance Grout (VHPG) for Repairing Materials. Institut Teknologi Sepuluh Nopember (2018).

[23] V.M. Malhotra, V.S. Ramachandran, R.F. Feldman, P.-C. Aïtcin, Condensed Silica Fume in Concrete. CRC Press (2018).

[24] G. Vijayakumar, M.H. Vishaliny, D. Govindarajulu, Studies on Glass Powder as Partial Replacement of Cement in Concrete Production. Int. J. Emerg. Technol. Adv. Eng. **3**, 2, 153-157 (2013).

[25] R.U.D. Nassar, P. Soroushian, Strength and durability of recycled aggregate concrete containing milled glass as partial replacement for cement. Constr. Build. Mater. **29**, 368-377 (2012). DOI: https://doi.org/10.1016/j.conbuildmat.2011.10.061

[26] N.A. Soliman, A. Tagnit-Hamou, Development of ultra-high-performance concrete using glass powder – Towards ecofriendly concrete. Constr. Build. Mater. **125**, 600-612 (2016). DOI: https://doi.org/10.1016/j.conbuildmat.2016.08.073

[27] K. Wille, A.E. Naaman, S. El-Tawil, G.J. Parra-Montesinos, ultra-high performance concrete and fiber reinforced concrete: Achieving strength and ductility without heat curing. Mater. Struct. Constr. **45**, 309-324 (2012). DOI: https://doi.org/10.1617/s11527-011-9767-0

[28] M.A. Moghadam, R.A. Izadifard, Experimental investigation on the effect of silica fume and zeolite on mechanical and durability properties of concrete at high temperatures. SN Appl. Sci. **1**, 6, 682 (2019). DOI: https://doi.org/10.1007/s42452-019-0739-2

[29] S. Abbas, M.L. Nehdi, M.A. Saleem, Ultra-High Performance Concrete: Mechanical Performance, Durability, Sustainability and Implementation Challenges. Int. J. Concr. Struct. Mater. **10**, 3, 271-295 (2016). DOI: https://doi.org/10.1007/s40069-016-0157-4

[30] K. Wille, A.E. Naaman, G.J. Parra-Montesinos, Ultra-High Performance Concrete with Compressive Strength Exceeding 150 MPa (22 ksi): A Simpler Way. ACI Mater. J. **108**, 1, 46-54 (2011). DOI: https://doi.org/10.14359/51664215

[31] P.-C. Aïtcin, Water and its role on concrete performance. In Science and Technology of Concrete Admixtures, Elsevier, pp. 75-86 (2016).

[32] J.J. Ekaputri, K. Maekawa, T. Ishida, Experimental Study on Internal RH of BFS Mortars at Early Age. Mater. Sci. Forum **857**, 305-310, May (2016). DOI: https://doi.org/10.4028/www.scientific.net/MSF.857.305

[33] ACI Committee 209, "ACI Fall 2015 Convention – Creep and Shrinkage in Concrete," Denver (2015).

[34] J.J. Ekaputri, T. Ishida, K. Maekawa, Autogeneous Shrinkage of Mortars Made With Different Types of Slag Cement. In Transaction of the Japan Concrete Institute **32**, 1, 353-358 (2010).

[35] F. Hamidi, F. Aslani, Additive manufacturing of cementitious composites: Materials, methods, potentials, and challenges. Constr. Build. Mater. **218**, 582-609 (2019). DOI: https://doi.org/10.1016/j.conbuildmat.2019.05.140

[36] J.J. Ekaputri, S. Junaedi, Wijaya, Effect of Curing Temperature and Fiber on Metakaolin-based Geopolymer. In Procedia Engineering **171**, 572-583 (2017). DOI: https://doi.org/10.1016/j.proeng.2017.01.376

[37] J.J. Ekaputri, C. Fujiyama, N. Chijiwa, T.D. Ho, H T. Nguyen, Improving Geopolymer Characteristics with Addition of Poly-Vinyl Alcohol (PVA) Fibers. Civ. Eng. Dimens. **23**, 1, 28-34 (2021). DOI: https://doi.org/10.9744/CED.23.1.28-34

[38] J.J. Ekaputri, H. Limantono, Triwulan, T.E.S. Susanto, M.M.A.B. Abdullah, Effect of PVA fiber in increasing mechanical strength on paste containing glass powder. Key Eng. Mater. **673**, 83-93 (2016). DOI: https://doi.org/10.4028/www.scientific.net/KEM.673.83

[39] Z. Malaeb, H. Hachem, A. Tourbah, T. Maalouf, N. El Zarwi, F. Hamzeh, 3D Concrete Printing: Machine and Mix Design. Int. J. Civ. Eng. Technol. **6**, 6, 14-22 (2015).

[40] ASTM International, ASTM C143-15: Standard Test Method for Slump of Hydraulic-Cement Concrete, pp. 1-4 (2015).

[41] ASTM International, ASTM C230-08:Standard Specification for Flow Table for Use in Tests of Hydraulic Cement. (2008).

[42] ASTM International, ASTM C403-16: Standard Test Method for Time of Setting of Concrete Mixtures by Penetration Resistance. pp. 1-7 (2016).

[43] ASTM International, ASTM C496-17: Standard Test Method for Splitting Tensile Strength of Cylindrical Concrete Specimens, pp. 1-5 (2017).

[44] ASTM International, ASTM C39-20: Standard Test Method for Compressive Strength of Cylindrical Concrete Specimens, pp. 1-8 (2020).

[45] H. Limantono, J.J. Ekaputri, T.E. Susanto, Effect of silica fume and glass powder on high-strength paste. Key Eng. Mater. **673**, 37-46 (2016). DOI: https://doi.org/10.4028/www.scientific.net/KEM.673.37

[46] H. Du, K.H. Tan, Properties of high volume glass powder concrete. Cem. Concr. Compos. **75**, 22-29 (2016). DOI: https://doi.org/10.1016/j.cemconcomp.2016.10.010

[47] R.J.M. Wolfs, F.P. Bos, T.A.M. Salet, Hardened properties of 3D printed concrete: The influence of process parameters on interlayer adhesion. Cem. Concr. Res. **119**, February, 132-140 (2019). DOI: https://doi.org/10.1016/j.cemconres.2019.02.017

[48] C.A. Juarez, G. Fajardo, S. Monroy, A. Duran-Herrera, P. Valdez, C. Magniont, Comparative study between natural and PVA fibers to reduce plastic shrinkage cracking in cement-based composite. Constr. Build. Mater. **91**, 164-170 (2015). DOI: https://doi.org/10.1016/j.conbuildmat.2015.05.028